Nuclear Data Relevant to the Production of the Positron Emitting Technetium Isotope ^{94m}Tc via the ^{94}Mo(p,n)-reaction

By F. Rösch and S. M. Qaim

Institut für Nuklearchemie, Forschungszentrum Jülich GmbH, D-52425 Jülich, Germany

p-induced nuclear reaction | Stacked-foil technique | Excitation function | Positron emitter ^{94m}Tc | Isomeric cross section ratio

Summary

Excitation functions were measured by the stacked-foil technique for ^{94}Mo(p,xn)^{94m,94g,93m,93m,g}Tc-reactions from threshold to 18.4 MeV. Thin samples of 93.9% enriched ^{94}Mo powder of 10 mm diameter and 3–6 mg/cm^2 thickness were prepared via a sedimentation method. Thick target yields of ^{94m}Tc were calculated from the measured excitation function, and the levels of radiotechnetium impurities were determined experimentally. The optimum proton energy range for the production of ^{94m}Tc was found to be $E_p = 13 \rightarrow 7$ MeV, with the expected thick target yield of 54 mCi (2 GBq)/µAh. The isomeric cross section ratio for the isomeric pair ^{94m,g}Tc is discussed.

Introduction

Due to the ideally suitable nuclear decay properties of ^{99m}Tc, its convenient availability in a commercial generator form and the recent progress in both the Tc-radiopharmaceutical chemistry and the SPECT imaging techniques, [^{99m}Tc]-radiopharmaceuticals play a dominant role in nuclear medical diagnosis. To quantify the biodistribution of these radiopharmaceuticals in humans, however, it would be meaningful to combine SPECT and PET by using a positron emitting Tc-isotope for the corresponding PET measurements. Taking advantage of the modern PET technique, the data obtained on the quantification of uptake kinetics and their mechanisms would allow a better estimate of the diagnostic potential of new [^{99m}Tc]-compounds. Furthermore, it should be possible to quantify models on the metabolic pathways of already established [^{99m}Tc]-radiopharmaceuticals.

Among the neutron deficient technetium isotopes, ^{94m}Tc seems to be the most suitable isotope. It has a half-life of 52 min, a β^+ branching of 70%, and a positron end point energy of 2.47 MeV. Recently, first experiments on the practical production yields of ^{94m}Tc were done in irradiations of natural molybdenum with 13.5 MeV protons and 13 MeV deuterons [1] as well as with 11 MeV protons [2–4]. The basic nuclear data for these production routes are unknown. The aim of this work was to determine the nuclear data relevant to the production of ^{94m}Tc via the ^{94}Mo(p,n)-

reaction, and to measure the experimental thick target yields as well as the level of isotopic impurities.

Experimental

Excitation functions were measured by the conventional stacked-foil technique as described in earlier publications from this institute, cf. [5–7]. Some of the salient features relevant to the present work are discussed below.

Target material

^{94}Mo was used as target material, commercially supplied as metal powder by Oak Ridge National Laboratory, USA. The isotopic composition was: ^{92}Mo (0.87%), ^{94}Mo (93.9%), ^{95}Mo (2.85%), ^{96}Mo (1.04%), ^{97}Mo (0.40%), ^{98}Mo (0.75%), ^{100}Mo (0.22%). The chemical purity was specified by the supplier as >99.1% molybdenum. Small portions of the material were converted to obtain ^{94}MoO$_3$ by means of thermal and dry oxidation in a quartz tube at about 850°C in order to check both the metallic and the oxide forms of the enriched molybdenum for the preparation of thin samples.

Sample preparation

Thin samples of enriched ^{94}Mo were prepared by means of a special sedimentation method. Details of this procedure were described in [8]. In brief, suspensions of very fine ^{94}Mo or ^{94}MoO$_3$ powder in water-free acetone were prepared by mixing and stirring. Small amounts of collodium (cellulose nitrate) were added (0.5% in the case of the metallic form, 3% in the case of the oxide form). Aliquots of about 200–300 µl of these solutions were transferred to a vertical cylindrical vessel (10 mm diameter) held vertically in a PTFE device. A 13 mm diameter copper foil (25 µm thick) was placed at the open bottom of the cylinder. The acetone of the suspension was allowed to evaporate slowly. The copper foil and the empty PTFE cylinder were then carefully separated from each other. Homogeneous and mechanically stable samples of thicknesses in the order of 3–6 mg/cm^2 (Mo metal) and 5–10 mg/cm^2 (MoO$_3$) were obtained on the sur-

face of the copper backing foil. Samples in both the chemical forms were found to be suitable for the stacked-foil irradiations, but finally the Mo metal samples were selected. To avoid contamination, the surface of each sample was covered with a 10 μm thick Al foil, having the same diameter of 13 mm as the Cu backing foil. The samples thus prepared had a sandwich form. Additionally, for yield measurements thicker targets with 33 – 162 mg/cm² of ^{94}Mo were prepared using the same technique.

Irradiations

Several stacks, each containing 6 – 8 sandwiched samples, were irradiated at the Jülich compact cyclotron CV28, each for 15 min at a beam current of 100 nA. For measurements below 8 MeV, where the cross sections are relatively low, an extra irradiation of 3 samples was done for 60 min at 200 nA. In preliminary experiments, a few identically prepared samples consisting of natural molybdenum were irradiated.

Each stack contained on the front side a separate Cu monitor foil (25 μm thick). The primary incident proton energy was determined to be 19.2 MeV via the ratio $\sigma_{(p,2n)}/\sigma_{(p,n)}$ of the monitor reactions ^{63}Cu(p,2n)^{62}Zn and ^{63}Cu(p,n)^{63}Zn, as a function of the proton energy, cf. [7]. The proton beam current was determined via the ^{63}Cu(p,n)^{63}Zn-reaction, cf. [9, 10]. Here, the ^{63}Zn activity produced within the Cu backing foil of each ^{94}Mo sample could be used. For measurement of thick target yields and isotopic impurities, 1 h irradiations at 45 – 200 nA were done.

Measurement of radioactivity

The activity of each sample and the monitor foil was determined by γ-ray spectrometry using a 35 cm³ Ge(Li) detector coupled to an Ortec (Spectrum ACE) 4 K MCA Plug-In Card. The card was connected to an IBM-compatible PC-AT. Peak area analysis was done using Maestro II MCA emulation software. The detector counting efficiencies for different photon energies and counting distances were determined using calibrated standard sources (errors < 3%) obtained from PTB Braunschweig and Amersham International.

The radioactivity was measured non-destructively, i.e. the ^{94}Mo samples on Cu backing foils together with the Al covers were counted without a mechanical removal of the covering foil or chemical treatment of the target material. With respect to cross section measurements, counting was performed within two days after the irradiations, and attention was paid exclusively to the short-lived Tc isotopes 94m and 94g as products of the ^{94}Mo(p,n)-process and to 93m and 93g as products of the ^{94}Mo(p,2n)-reaction at higher particle energies. Within the same interval of measurements the monitor reaction products ^{62,63}Zn were de-

Table 1. Decay data of the product nuclei used in the present study, cf. [11]

Nuclide	Mode of decay (%)	$T_{1/2}$	E_γ (keV)	Abundance γ (%)
^{94m}Tc	β^+ (70)	52 min	992.8	2.3
	EC (30)		1868.3	5.7
^{94g}Tc	β^+ (11)	4.88 h	702.6	99.6
	EC (89)		916.1	7.6
^{93m}Tc	IT (80)	43.5 min	392.5	60
	EC (20)			
^{93g}Tc	EC (88.6)	2.75 h	1363.1	66
	β^+ (11.4)			
^{63}Zn	β^+ (93)	38.1 min	669.8	8.4
	EC (7)		962.6	6.6
^{62}Zn	EC (93.1)	9.26 h	548.4	15.2
	β^+ (6.9)		596.7	25.7

termined. The decay data used in the γ-ray spectroscopy of the radioisotopes investigated are summarized in Table 1, cf. [11]. In particular, for ^{94m}Tc, γ-ray energies with relatively low abundances were chosen. This is because the dominant γ-rays of this isotope occur also in the decay of other technetium isotopes present in the irradiated samples.

Calculation of cross sections and errors

The count rates were corrected for pile-up losses as well as for γ-ray abundances and the efficiencies of the detector. The errors due to random coincidences were kept small by choosing a sample to detector distance such that the dead time was < 7%. Since the distance between the sample and the detector was always > 10 cm, the correction for real coincidence losses was negligible. The cross sections were calculated using the well-known activation formula. The overall uncertainties in the cross sections were obtained by taking the square root of the sum of the squares of the individual errors. The individual errors considered were as follows:

– Target thickness (~2%).
– Inhomogeneity in target thickness (<10%).
– Bombarding proton beam intensity (<10%).
– Detector efficiency and sample-detector geometry (~5%).
– Statistical errors (0.5 – 10%; for energy points near the threshold up to 20%).
– Decay data errors (<3%; except for ^{94m}Tc, where due to the use of low abundance γ-rays an error of 5% was adopted).

For the ^{94}Mo(p,xn)-reactions the typical overall errors are < 20% over almost the whole energy range, with the exception of the threshold region where the errors are 20 – 40%. For the ^{nat}Mo(p,xn)-experiments the corresponding errors are twice as high. The error of the isomeric cross section ratio is less than 10%

Table 2. Cross sections for the formation of ^{94m}Tc, ^{94g}Tc, ^{93m}Tc and ^{93m,g}Tc in proton induced nuclear reactions on highly-enriched ^{94}Mo and isomeric cross section ratio of the isomeric pair ^{94m,g}Tc as $R = \sigma^{94m}\text{Tc}/\sigma^{94m+g}\text{Tc}$

E_p (MeV)	$\sigma^{94m}\text{Tc}^*$ (mb)	$\sigma^{94g}\text{Tc}^*$ (mb)	$\sigma^{93m}\text{Tc}^*$ (mb)	$\sigma^{93m,g}\text{Tc}^{**}$ (mb)	$\sigma^{93g}\text{Tc}^*$ (mb)	$R = \dfrac{\sigma^{94m}\text{Tc}}{\sigma^{94m+g}\text{Tc}}$
18.4	47.0±8.5	45.6±7.4	88.2±13.5	372.0±49.2	301±51	0.508
18.1	50.6±16.4	51.0±13.3	81.9±13.2	450.4±57.2	385±59	0.498
17.6	67.8±17.7	55.6±6.9	62.2±11.7	255.4±39.0	206±41	0.549
17.4	69.4±11.0	66.7±9.8	76.9±12.9	319.4±49.9	258±52	0.510
16.5	109.2±17.3	80.9±10.8	38.2±4.9	226.9±36.9	196±37	0.574
16.2	196.1±53.3	105.0±14.3	50.7±11.9	280.4±49.2	240±51	0.651
15.4	222.2±114.0	144.4±22.8	23.7±5.6	131.8±36.7	113±37	0.606
15.1	241.9±32.0	143.0±17.8	13.9±2.7	114.9±14.3	104±15	0.629
14.3	369.4±49.0	172.3±25.8	6.5±3.3	10.4±1.9	99±19	0.682
14.0	391.9±58.1	149.4±18.6	1.1±0.3	3.9±1.1	38±11	0.724
13.1	458.7±59.0	172.7±25.8				0.727
12.4	432.6±61.3	131.7±17.4				0.767
11.9	455.5±65.2	127.1±16.2				0.782
11.2	434.2±82.7	103.4±19.0				0.808
10.4	371.3±50.5	86.8±14.0				0.811
9.6	363.5±50.7	69.3±10.6				0.840
9.3	349.2±55.2	62.4±9.4				0.848
8.8	339.7±66.8	47.5±14.3				0.877
8.3	230.0±45.4	32.0±10.8				0.878
7.9	144.3±21.7	13.0±3.2				0.917
7.6	119.5±20.3	18.6±4.9				0.865
7.2	60.5±20.3	6.5±3.0				0.902
6.9	32.0±30.0	3.0±2.0				0.914
6.1	2.0±1.5	0.2±0.2				0.909

* Independent formation cross section.
** Cumulative cross section for the formation of 2.75 h ^{93g}Tc.

since the cross section values of both the metastable and ground states were derived from the same irradiation of the same samples. In this case, uncertainties in the beam intensity and target homogeneity did not contribute.

The average proton energy degradation within one ^{94}Mo sample was 0.1 MeV. The uncertainties in the energy scale are estimated to increase from 0.15 MeV at $E_p = 18$ MeV to 0.30 MeV at $E_p = 7$ MeV.

Results and discussion

Cross section data and theoretical thick target yields

The measured cross sections of the ^{94}Mo(p,xn)-reactions are given in Table 2. The values for ^{94m}Tc, ^{94g}Tc and ^{93m}Tc give direct production cross sections. The data for ^{93m,g}Tc, on the other hand, describe the cumulative formation cross sections of the 2.75 h ^{93g}Tc since the ^{93m}Tc decays 80% by IT to ^{93g}Tc. For these measurements a cooling time of 4 h was necessary to allow complete decay of ^{93m}Tc. To be complete, "pure" σ^{93g}Tc-data were calculated from the experimental data according to $\sigma^{93g}\text{Tc} = \sigma^{93m+g}\text{Tc} - 0.8\sigma^{93m}\text{Tc}$. The results are also included in Table 2 and describe the independent formation cross sections of this radioisotope.

The excitation functions of the ^{94}Mo(p,n)^{94m,94g}Tc reactions over the most relevant proton energy region between 6 and 19 MeV and of the

^{94}Mo(p,2n) ^{93m,93m,g}Tc reactions between 13 and 19 MeV have been measured for the first time using enriched target isotope. In the lowest proton energy region the σ-values for the ^{94}Mo(p,n)-reaction can be compared with some experimental results, reported by Skakun et al. [12] over the proton energy range of 5.5 to 9.0 MeV, using enriched molybdenum. Most of the other papers dealing with Mo(p,xn)-reactions (x = 1−4) describe practical yields of various other technetium isotopes. Excitation functions have thus been studied in the context of production of ^{95m}Tc, ^{96}Tc, ^{98}Tc and ^{99m}Tc by proton bombardment of natural molybdenum only [12−19].

Our data are shown in Fig. 1 with eye-guided curves. The (p,n)-reaction leading to the formation of ^{94m}Tc starts at a threshold energy of about 6 MeV and reaches a maximum cross section of 480 mb at about 12 MeV. The ^{94g}Tc product is formed simultaneously, but with significantly lower cross sections. The results of Skakun et al. [12] are included for comparison. Except for an energy shift of about 1 MeV those data are in agreement with our values.

Due to inherent large errors we did not show our results obtained from irradiations of natural molybdenum. In any case, at $E_p > 13$ MeV the ^{95}Mo(p,2n)-reaction contributes increasingly to the formation of ^{94m}Tc. Accurate ^{94m}Tc formation cross sections could thus be obtained only using highly enriched ^{94}Mo.

At a proton energy higher than 12 MeV, the (p,2n)-process on ^{94}Mo also occurs, leading to the two products ^{93m}Tc and ^{93g}Tc. Maximum cross section values
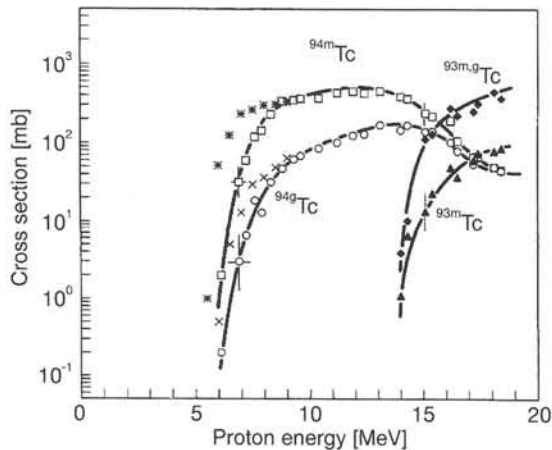
Fig. 1. Excitation functions of ^{94}Mo(p,xn)-processes leading to the formation of ^{94m}Tc, ^{94g}Tc, ^{93m}Tc, ^{93m,g}Tc. The values for ^{93m,g}Tc describe the cumulative formation cross section for the 2.75 h ^{93g}Tc. Typical error bars in different energy regions are given. Some literature data [12] are also included ($*$, $\times$).
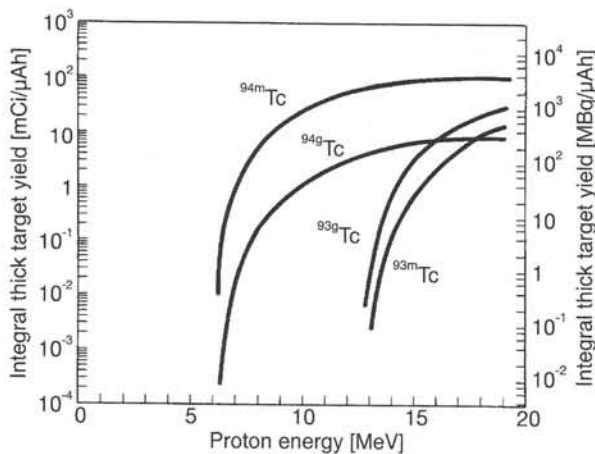

Fig. 3. Isomeric cross section ratio $R = \sigma^{94m}\text{Tc}/\sigma^{94m+g}\text{Tc}$ in the ^{94}Mo(p,n)-process as a function of the proton energy. The literature values for the ^{94}Mo(p,n) reaction [12] as well as the ^{96}Mo(p,3n)-process [21, 22] are also shown.

Fig. 2. Integral thick target yields of ^{94m}Tc, ^{94g}Tc, ^{93m}Tc and ^{93g}Tc calculated from the excitation functions of ^{94}Mo(p,xn)-processes, given in Fig. 1. The curve for ^{93g}Tc is based on the independent cross section values given in Table 2.

for these processes were observed at the maximum effective proton energy of 18.4 MeV in the first sample, but obviously the (p,2n)-process increases further with increasing particle energy.

Yields of the different Tc-isotopes at EOB were calculated from the experimentally measured excitation functions and the stopping powers and ranges for protons in molybdenum as tabulated by Williamson et al. [20]. The integral thick target yields are shown in Fig. 2. From the excitation functions and yield curves it is evident that the maximum yield of ^{94m}Tc would be obtained over the energy range of $E_p = 15 \rightarrow 9$ MeV. Integral thick target yields over this energy range would be 75.5 mCi (2.8 GBq)/μAh for ^{94m}Tc and 5.2 mCi (190 MBq)/μAh for ^{94g}Tc.

Isomeric cross section data

A consideration of the formation of the isomeric pair ^{94m,g}Tc is important with respect to the level of ^{94g}Tc
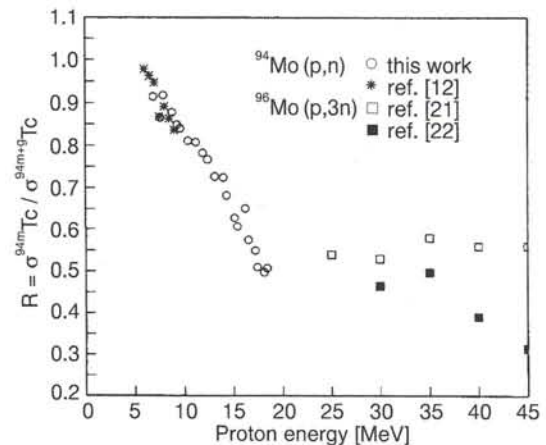
as an isotopic impurity in ^{94m}Tc. Moreover, the role of nuclear spin in the deexcitation of a compound nucleus is of special interest. So the cross section ratio of this isomeric pair was studied in more detail. In the present case, the metastable and the ground states have spins of 2^+ and 7^+, respectively. Cross sections obtained experimentally are higher for ^{94m}Tc than for ^{94g}Tc. On the other hand, the isomeric cross section ratio is strongly dependent on the incident proton energy, the amount of ^{94g}Tc increasing at high proton energies. The ratio $R = \sigma^{94m}\text{Tc}/\sigma^{94m+g}\text{Tc}$ is shown graphically in Fig. 3. The highest values of R were found for low proton energies. At $E_p = 7$ MeV for example, this ratio is 0.9, indicating that almost 90 per cent of the ^{94m,g}Tc formed is represented by the metastable state ^{94m}Tc. The isomeric cross section ratio decreases with the increasing proton energy and reaches a level of about 0.5 at the highest proton energy investigated in this work (~ 18 MeV), reflecting a 1:1 formation of the metastable and ground state isomers.

These results are compared with the data given by Skakun et al. [12] for the ^{94}Mo(p,n)^{94m,g}Tc-reaction at the lowest energies and by Hogan [21] and Vishnevskiy et al. [22] for the ^{96}Mo(p,xn)^{94m,94g}Tc-process at higher proton energies up to 65 and 70 MeV, respectively; cf. Fig. 3. Over the proton energy range of 5.5 to 9.0 MeV the literature and our isomeric cross section ratios agree very well. The other values, obtained at higher proton energies and for another nuclear reaction route, are also similar. It may be concluded phenomenologically, that the isomeric cross section ratio for this pair depends on the energy of the bombarding protons.

From the foregoing discussion it is evident, that for the production of ^{94m}Tc of maximum isotopic purity low proton energies should be preferred. Experimentally determined isotopic impurity of ^{94g}Tc in a 1 h irradiation in the low energy region of $E_p < 10$ MeV is 5.5% at EOB, reaching levels of about 10 to 20% at 1
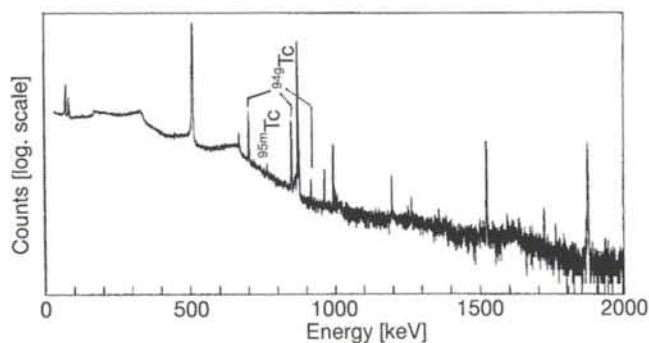
Fig. 4. γ-ray spectrum of "pure" ^{94m}Tc (with 5% ^{94g}Tc). The γ-rays of technetium isotopes other than ^{94m}Tc are indicated. All the other γ-rays belong to ^{94m}Tc.

Fig. 5. Levels of ^{94g}Tc, ^{93m}Tc and ^{93m,g}Tc isotopic impurities as a function of the proton energy (calculated from the experimentally obtained yields for 15 min irradiations of thin samples of 93.9% enriched ^{94}Mo), relative to ^{94m}Tc = 100.

to 2 hours after EOB, which seem to be realistic periods to start medical applications of [^{94m}Tc]-labelled compounds. Longer irradiations, of course, will lead to somewhat higher amounts of ^{94g}Tc. (For a detailed discussion on the time-dependent change in the percentages of ^{94m}Tc and ^{94g}Tc activities see below.) To measure a ^{94m}Tc γ-ray spectrum as pure as possible, ^{94}Mo was irradiated with 9 MeV protons for 15 min. The spectrum was recorded at 15 min after EOB and is shown in Fig. 4; the "pure" ^{94m}Tc γ-spectrum has only 5% ^{94g}Tc.

Impurities and experimental thick target yields

Five categories of radionuclidic impurities may occur in ^{94m}Tc. Firstly, as discussed above, ^{94g}Tc, which is formed simultaneously with ^{94m}Tc, is the main isotopic impurity at least at $E_p < 14$ MeV. Secondly, there are various technetium isotopes, originating from (p,xn)-reactions on stable molybdenum isotopes other than ^{94}Mo, i.e. $^{92,95,96,97,98 \text{ and } 99}$Mo. However, most of them are present within the enriched ^{94}Mo target at a concentration about 100 fold lower than that of ^{94}Mo. The only important Mo isotope in this context is ^{95}Mo with an abundance of 2.85%, yielding ^{95m}Tc ($T_{1/2} = $ 61 d) and ^{95g}Tc ($T_{1/2} = 20.0$ h) at $E_p < 15$ MeV, and additionally ^{94m,94g}Tc at higher proton energies. Thirdly, there is the ^{94}Mo(p,2n)-process, producing the ^{93m,g}Tc isotopes as the most relevant radionuclidic impurities at proton energies above 13 MeV. In practice, however, the ^{94}Mo(p,2n)-contribution is minimized by choosing the production energy region of $E_p < 14$ MeV. Fourthly, there are other proton-induced nuclear reactions on ^{94}Mo, leading to non-technetium isotopes, e.g. ^{94}Mo(p,pn)^{93m}Mo and ^{94}Mo(p,α)^{91}Nb. In fact, ^{93m}Mo ($T_{1/2} = 6.85$ h) was detected experimentally in the irradiated ^{94}Mo samples, in particular at proton energy > 14 MeV. The last group of radionuclidic impurities may arise from chemical impurities in the ^{94}Mo-target material used for irradiations. The latter two types of impurities are neglected in this paper, since those impurities
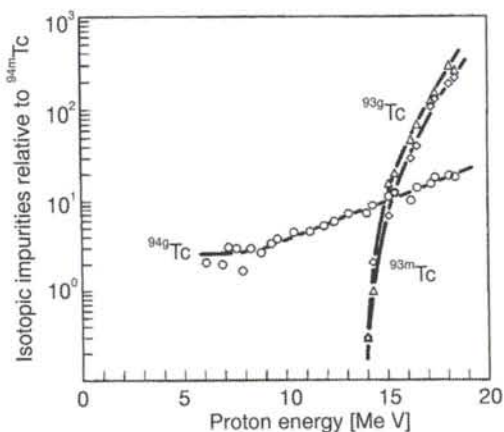
should be removed in the chemical separation of ^{94m}Tc.

The isotopic impurities ^{94g}Tc, ^{93m}Tc and ^{93m,g}Tc (at EOB of 15 min irradiations) are shown in Fig. 5. To minimize the levels of these impurities, in the production of ^{94m}Tc an energy range of $E_p = 13 \to 7$ MeV should be preferred. Under practical conditions of 1 hour irradiations over this energy range the levels of the three impurities amount to 5.5%, 0.04% and 0.17%, respectively, as against 6.9%, 0.37% and 1.6% in the higher energy range of $E_p = 15 \to 8$ MeV. Although also the latter level of isotopic impurities seems to be acceptable, one has to consider the increase in the level of impurities with the decay time after EOB. (With realistic periods of one or two half-lives of ^{94m}Tc, the ^{93g}Tc impurity will reach values of 3 to 6% in the case of the higher energy range instead of 0.3 to 0.6% in the lower energy range.)

The isotopic impurities were also studied experimentally in two thick target experiments. In one experiment 162 mg/cm^2 ^{94}Mo was irradiated at $E_p = 13 \to 10$ MeV, i.e. within the optimum proton energy range for the production of ^{94m}Tc, for 1 hour at 45 nA. In another experiment, 33 mg/cm^2 ^{94}Mo was irradiated at $E_p = 18.4 \to 17.5$ MeV for 1 hour at 200 nA. Both targets were measured for a long period after the decay of ^{94m,g}Tc. The isotopic impurities found are summarized in Table 3. The experimental thick target yields obtained over the optimum energy range were compared with the theoretical ones. The experimental parameters were, however, only semi-realistic production parameters since the beam intensity was relatively low. The theoretically expected thick target yield of 1.8 mCi (67 MBq) ^{94m}Tc agreed exactly with the experimental value.

Comparison of production data obtained using highly enriched ^{94}Mo and natural molybdenum targets

In the literature, experimental thick target yields of ^{94m}Tc are reported only for natural molybdenum tar-

Table 3. Isotopic impurities in ^{94m}Tc produced in irradiations of highly enriched ^{94}Mo and natural molybdenum with protons. The numbers are relative to ^{94m}Tc assumed as 100

E_p (MeV)	Reference time	Isotopic impurities relative to ^{94m}Tc assumed as 100							
		^{93m,g}Tc	^{93m}Tc	^{94g}Tc	^{95g}Tc	^{95m}Tc	^{96g}Tc	^{96m}Tc	^{99m}Tc
18.4→17.5	EOB*	270	164	22	—	—	—	—	—
	EOB**	240	180	24	0.3	0.005	0.01	—	0.1
	EOB+2h**	720	130	90	1.4	0.003	0.05	—	0.4
15→8	EOB*	0.17	0.04	5.5	—	—	—	—	—
14→7	EOB*	0.37	0.31	6.1	—	—	—	—	—
13→7	EOB*	1.6	0.37	6.9	—	—	—	—	—
13→10	EOB*	<0.01	<0.01	9.7	0.2	<0.01	0.02	<0.01	0.02
	EOB+2h*	<0.01	<0.01	36.2	1.0	0.01	0.1	<0.01	0.08
	EOB**	<0.01^n	<0.01^n	16.7^n	12.8^n	0.07^n	2.7^n	100^n	7.2^n
	EOB+2h**	<0.01^n	<0.01^n	62.1^n	59.0^n	0.4^n	13.0^n	99^n	28.4^n
9.5	EOB*	—	—	4.1	—	—	—	—	—
	EOB**	<0.01	<0.01	4.1	0.24	0.004	0.02	<0.01	0.005
	EOB+2h**	<0.01	<0.01	15.28	1.11	0.02	0.09	<0.01	0.02

*   Deduced from theoretical thick target yields for ^{94g}Tc, ^{93m}Tc and ^{93m,g}Tc.
** Experimental results.
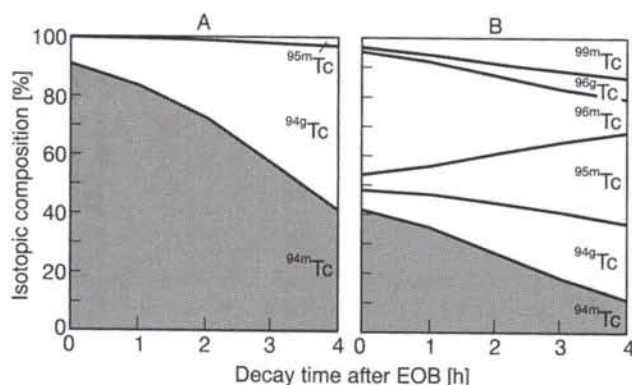^{n} Natural molybdenum target.

Fig. 6. Isotopic composition of radiotechnetium resulting from a 1 hour irradiation of (A) 93.9% enriched ^{94}Mo and (B) of natural molybdenum at $E_p = 13 \rightarrow 10$ MeV, shown as a function of decay time after EOB.

gets. For the energy range $E_p = 11 \rightarrow 6$ MeV the yield of ^{94m}Tc was measured as 7 mCi (259 MBq)/μA at saturation, with 34% ^{94g}Tc-content [2]. For a 53 min irradiation and a chemical procedure lasting 53 min after EOB, a yield of 1.8 mCi (67 MBq) ^{94m}Tc, with 14% ^{94g}Tc, was given [2, 3]. Irradiation of 150 mg/cm^2 ^{nat}MoO$_3$ in the energy range of $E_p = 13 \rightarrow 11$ MeV resulted in 2 mCi (74 MBq)/μAh ^{94m}Tc and 6.6% ^{94g}Tc at EOB [1]. These practical yields using natural molybdenum targets would be sufficient from the point of view of absolute ^{94m}Tc activity but not regarding its quality. Taking into account the level of isotopic impurities, this production route cannot be recommended. To illustrate this fact, Table 3 includes the isotopic composition of the radiotechnetium under identical irradiations. Fig. 6 illustrates graphically the isotopic composition of the radiotechnetium fractions if both 93.9% enriched ^{94}Mo and natural Mo targets

were irradiated under identical conditions at $E_p = 13 \rightarrow 10$ MeV for one hour. At EOB and at two hours after EOB (again to take a realistic time with respect to potential nuclear medical application of [^{94m}Tc]radiopharmaceuticals), the ^{94m}Tc amounts to 90 and 73 per cent in the case of the enriched ^{94}Mo and to 41 and 26 per cent in the case of natural molybdenum, respectively. With respect to quantitative PET-measurements, generally speaking, the overall rate of positron emission within the radiotechnetium fraction from the natural molybdenum target is almost only half of that from the enriched ^{94}Mo target. Despite some possible problems in correct quantitative PET measurements, the lower β^+ percentages seem to be still sufficient, but the radiation dose to the patients is significantly higher. In any case, ^{94m}Tc produced using highly enriched ^{94}Mo is superior.

Conclusion

The ^{94}Mo(p,n)-process on highly enriched ^{94}Mo offers suitable possibilities for the production of the positron-emitter ^{94m}Tc. This was demonstrated by studying the excitation functions of ^{94}Mo(p,xn)-processes, and by measuring the experimental thick target yields as well as the isotopic impurities. The optimum proton energy range for the ^{94m}Tc production is $E_p = 13 \rightarrow 7$ MeV, indicating that small-sized cyclotrons are adequate. ^{94m}Tc yields of 54 mCi (2 GBq)/μAh over this energy range are relatively high. The main isotopic impurity is the ^{94}Tc ground state isomer, with the isomeric cross section ratio σ^{94m}Tc:σ^{94g}Tc varying from 10:1 at $E_p = 7$ to 1:1 at 18 MeV. Over the optimum proton energy range the level of ^{94g}Tc at EOB after a one hour irradiation amounts to 5.5%.

Acknowledgements

References

1. Rösch, F., Beyer, G.-J.: Längerlebige Positronemitter: Einzelnuklide und Geneatorsysteme, Produktion am Rossendorfer Zyklotron U-120, radiochemische Studien und Möglichkeiten für die PET. Report ZfK-771 (1991).
2. Nickles, R. J., Nunn, A. D., Stone, C. K., Perlmann, S. B., Levine, R. L.: Proceedings of the 38th Annual Meeting, Society of Nuclear Medicine, Cincinnati, June 1991; Abstracts: J. Nucl. Med. 32, 925 (1991).
3. Nickles, R. J., Christian, B. T., Martin, C. C., Nunn, A. D., Stone, C. K.: Proceedings of the 39th Annual Meeting, Society of Nuclear Medicine, Los Angeles, June 1992; Abstracts: J. Nucl. Med. 33, 850 (1992).
4. Nickles, R. J., Christian, B. T., Nunn, A. D., Stone, C. K.: IXth Int. Symp. Radiopharm. Chem., Paris, April 1992; Abstracts: J. Label. Comp. Radiopharm. 23, 447 (1993).
5. Weinreich, R., Schult, O., Stöcklin, G.: Int. J. Appl. Radiat. Isot. 25, 353 (1974).
6. Qaim, S. M., Stöcklin, G., Weinreich, R.: Int. J. Appl. Radiat. Isot. 28, 947 (1977).
7. Piel, H., Qaim, S. M., Stöcklin, G.: Radiochim. Acta 57, 1 (1992).
8. Rösch, F., Qaim, S. M., Stöcklin, G.: Radiochim. Acta 61, 1 (1993).
9. Colle, R., Kishore, R., Cumming, J. B.: Phys. Rev. C9, 1819 (1974).
10. Kopecky, P.: Int. J. Appl. Radiat. Isot. 36, 657 (1986).
11. Browne, E., Firestone, R. B.: Table of Radioactive Isotopes, (Ed. Shirley, V. S.), John Wiley and Sons, New York 1986.
12. Skakun, E. A., Batil, V. S., Rakivenkov, Y. N., Rastrepin, O. A.: Sov. J. Nucl. Phys. 46, 17 (1987).
13. Izumo, M., Matsuoka, H., Sorita, T., Nagame, Y., Sekine, T., Hata, K., Baba, S.: Appl. Radiat. Isot. 42, 297 (1991).
14. Hogan, J. J.: Phys. Rev. C6, 810 (1972).
15. Hogan, J. J.: J. Inorg. Nucl. Chem. 35, 705 (1973).
16. Hogan, J. J.: J. Inorg. Nucl. Chem. 35, 1429 (1973).
17. Kneef, D. W., Mann, F. M., Switkowski, Z. E.: Nucl. Phys. A250, 285 (1975).
18. Trufanov, A. M., Lovchikova, G. N., Salnikov, O. A., Simakov, S. P.: Sov. J. Nucl. Phys. 36, 299 (1982).
19. Almeida, G. L., Helus, F.: Radiochem. Radioanal. Lett. 28, 205 (1977).
20. Williamson, C. F., Boujot, J. P., Picard, J.: Tables of range and stopping power of chemical elements for charged particles of energy 0.5 – 500 MeV. Rapport CEA-R 3042 (1966).
21. Hogan, J. J.: J. Inorg. Nucl. Chem. 35, 2123 (1975).
22. Vishnevskiy, I. N., Zhelotonzhskiy, V. A., Lasko, T. N.: Sov. J. Nucl. Phys. 41, 910 (1986).